Lab on a Chip

View Online
Dynamic Article Links

Cite this: *Lab Chip*, 2011, **11**, 115

www.rsc.org/loc

**TECHNICAL NOTE**

# A multicellular spheroid formation and extraction chip using removable cell trapping barriers†‡

**Hye-Jin Jin,[a] Young-Ho Cho,*[a] Jin-Mo Gu,[ab] Jhingook Kim[ab] and Yong-Soo Oh[ac]**

***Received 21st June 2010, Accepted 13th September 2010***
**DOI: 10.1039/c0lc00134a**



This paper presents a multicellular spheroid chip capable of forming and extracting three-dimensional (3D) spheroids using removable cell trapping barriers. Compared to the conventional macro-scale spheroid formation methods, including spinning, hanging-drop, and liquid-overlay methods, the recent micro-scale spheroid chips have the advantage of forming smaller spheroids with better uniformity. The recent micro spheroid chips, however, have difficulties in extracting the spheroids due to fixed cell trapping barriers. The present spheroid chip, having two PDMS layers, uses removable cell trapping barriers, thereby making it easy to form and extract uniform and small-sized spheroids. We have designed, fabricated and characterized a 4 × 1 spheroid chip, where membrane cell trapping barriers are inflated at a pressure of 50 kPa for spheroid formation and are deflated at zero gauge pressure for simple and safe extraction of the spheroids formed. In this experimental study, the cell suspension of non-small lung cancer cells, H1650, is supplied to the fabricated spheroid chip in the pressure range 145–155 Pa. The fabricated spheroid chips collect the cancer cells in the cell trapping regions from the cell suspension at a concentration of $2 \times 10^6$ ml$^{-1}$, thus forming uniform 3D spheroids with a diameter of 197.2 ± 11.7 μm, after 24 h incubation at 5% $CO_2$ and 37°C environment. After the removal of the cell trapping barriers, the spheroids formed were extracted through the outlet ports at a cell inlet pressure of 5 kPa. The cells in the extracted spheroids showed a viability of 80.3 ± 7.7%. The present spheroid chip offers a simple and effective method of obtaining uniform and small-sized 3D spheroids for the next stage of cell-based biomedical research, such as gene expression analysis and spheroid inoculation in animal models.

## Introduction

Since three-dimensional (3D) cell culture systems provide more accurate *in vivo-like* microenvironments[1] compared to two-dimensional (2D) monolayer cell culture systems, uniform 3D spheroid formation is crucial for cell-based biomedical research and clinical studies.[19–24] In the anti-cancer drug screening and animal model experiments, for example, the 3D multicellular spheroids, resembling avascular tumor nodules, are used for basic biological research on the regulation of tumor cell proliferation, differentiation, and death processes, as well as for clinically relevant studies on micrometastases, intervascular tumors and chemoresistance.[25,26,28,29] Recent cancer research[2,17,18] also shows that gene expression in the 3D spheroids is much closer to clinical expression profiles than those observed in 2D monolayers. Thus, a simple and effective method for obtaining uniform 3D spheroids is required for gene expression analysis and cell inoculation in animal models.

The traditional macro-scale spheroid formation methods,[16,27] including spinning,[3] hanging drop,[4] and liquid-overlay[5] methods, are used to obtain 3D multicellular spheroids. The macro-scale methods form 3D spheroids from the cell suspensions based on the intercellular interactions in flasks and well-plates; thus having difficulties in forming uniform and small-sized (~200 μm) spheroids, which resemble avascular 3D cell–cell interactions.

Recently, the micro-scale spheroid formation chips[6–12] have been proposed for obtaining uniform and small-sized (10–300 μm) spheroids from cell suspensions trapped within fixed micro-structures, where the intercellular interactions are provided by forces such as centrifugal,[6,7] gravitational,[8] hydrodynamic,[9] and bio-chemical binding.[10–12] The micro spheroid chips,[6–12] however,

[a]*Cell Bench Research Center, KAIST, 373-1 Guseong-dong, Yuseong-gu, Daejeon, Republic of Korea 305-701. E-mail: semcell@kaist.ac.kr; Fax: +82-42-350-8690; Tel: +82-42-350-8691*
[b]*Cancer Research Center, Samsung Medical Center, 50 Ilwon-dong, Kangnam-gu, Seoul, Republic of Korea 135-710*
[c]*Central R&D Institute, Samsung Electromechanics Co, 314 Metan-3dong, Youngdong-gu, Suwon, Republic of Korea 443-743*

† Published as part of a LOC themed issue dedicated to Korean Research: Guest Editors: Professor Je-Kyun Park and Kahp-Yang Suh.
‡ Electronic supplementary information (ESI) available: Fig. S1 and S2. See DOI: 10.1039/c0lc00134a

show difficulties in growing and extracting the 3D spheroids due to the fixed cell trapping microstructures.

In this paper, we design, fabricate, and characterize a simple and effective micro-scale spheroid formation chip to form and extract 3D spheroids using removable cell trapping barriers. While the previous micro-scale spheroid chips use fixed cell trapping structures, the present spheroid chip uses removable cell trapping structures, thus making both spheroid formation and the extraction processes simple and safe. Furthermore, the present spheroid chip shows the possibility of being used for spheroid perfusion culture, since removable cell trapping structures give 3D spheroids space to grow.

## Design and analysis

### Spheroid chip

The 4 × 1 spheroid formation chip (Fig. 1a) consists of a cell inlet port and channels, a spheroid outlet port and channels, and four spheroid wells with the removable cell trapping barriers controlled by membrane pressure. The membrane pressure port of Fig. 1a is connected to the channels formed in the membrane pressure layer of Fig. 1b, while the cell inlet and the spheroid outlet of Fig. 1a are linked with the array of 4 spheroid wells prepared in the microfluidics layer of Fig. 1b.

In the spheroid wells of Fig. 1b and Fig. 1c, the cell trapping barriers are formed and removed respectively by the inflation (Fig. 1b) and the deflation (Fig. 1c) of the thin deformable membrane layer, sandwiched between the membrane pressure layer and the microfluidics layer. The use of the membrane layer as a valve originated from the Quake group.[13] The cell suspension, supplied to the cell inlet port of Fig. 1a, is distributed to 4 spheroid wells, while the pressure, supplied to the membrane pressure port of Fig. 1a, deflects the deformable membrane to form the horseshoe-shape cell trapping barriers inside the well. The inflated cell trapping barrier (Fig. 1b) collects the cells from the cell suspension to form a multicellular 3D spheroid. At reduced pressure, the deflated membrane (Fig. 1c) removes the cell trapping barrier, thus allowing the spheroid to exit to the spheroid outlet.

### Removable cell trapping barriers

We designed the diameter of the cell trapping region as 200 μm in order to obtain the 200 μm-diameter spheroids, widely used for drug screening.[14] We needed to decide the width and thickness of the cell trapping barrier such that the 200 μm-diameter cell trapping region is defined by the inner surfaces of the cell trapping barrier. The maximum height of the cell trapping barriers should cover the height (100 μm) of the spheroid wells in order to keep cells inside the cell trapping region. We decided to make the height of the spheroid well 100 μm to obtain the spheroids with the shape of an ellipsoid of revolution. If we need to form a sphere shape, we can adjust the height of the microfluidic channel to 200 μm and increase the membrane pressure to form higher cell trapping barriers. The maximum stress of the cell trapping barriers should be lower than the PDMS bonding strength of 7.1 MPa.[15] From the deflection and stress analysis of the PDMS membrane using COMSOL Multiphysics© simulation tool, we decided on the dimensions of the cell trapping barrier as shown in Fig. 1c, which satisfies the conditions mentioned above.

The deflection and stress simulation of the designed cell trapping barrier (Fig. S1, ESI‡), indicating that the 30 μm-thick and 300 μm-wide horseshoe-shape cell trapping barrier generates the maximum deflection of 99.7 μm (Fig. S1a, ESI‡) with a maximum stress of 5.61 MPa (Fig. S1b, ESI‡) at a membrane pressure of 50 kPa. As shown in Fig. 1c, the diameter of the spheroid well is designed to be 1 mm.



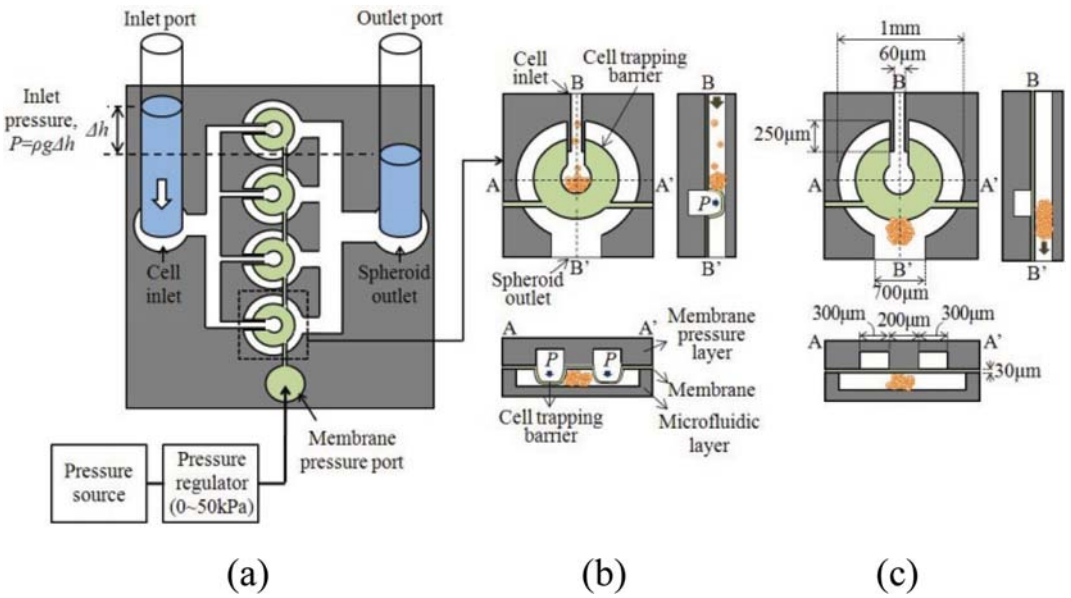


**Fig. 1** Spheroid formation and extraction in a spheroid well of the 4 × 1 spheroid chip using the removable cell trapping barriers: (a) top view of the spheroid chip; (b) the cell trapping barrier is formed for spheroid formation and incubation; and (c) the cell trapping barrier is removed for spheroid extraction.

 

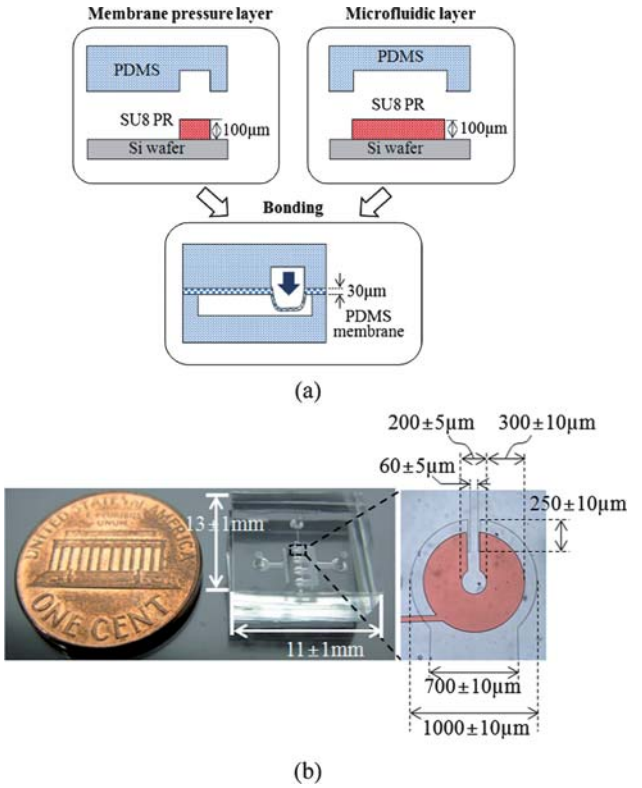


**Fig. 2** Fabrication of the spheroid chip: (a) fabrication process showing the cross section across B–B′ in Fig. 1b; (b) fabricated 4 × 1 spheroid chip and an enlarged spheroid well with the measured dimensions.

### Cell inlet guide channels

The inflated and deflated cell trapping barriers in the spheroid well (Fig. 1b and Fig. 1c) modify the fluidic resistance and the flow patterns between the cell inlet and the spheroid outlet. We analyzed the flow velocity and pattern near the entrance of the cell trapping barriers (Fig. S2, ESI‡) using the COMSOL Multiphysics© simulation tool based on a 3D fluid-structure interaction model of Fig. 1c. The inlet velocity vectors in Fig. S2a, ESI,‡ illustrate the influence of the inlet guide length on the flow patterns at the entrance of the cell trapping barriers, where the cell inlet pressure of 100 Pa is applied to the 100 μm-high horseshoe-shape cell trapping barrier in Fig. 1c. For the 100 μm-long inlet guide (Fig. S2a, ESI‡), the cells tend to go out of the cell trapping region rather than remain trapped inside the region due to the high fluidic resistance of the cell trapping barrier. We designed the length of the inlet guide to be 250 μm for an improved flow velocity pattern (Fig. S2b, ESI‡), suitable for cell trapping.

### Fabrication process

The fabrication process of the spheroid chip, illustrated in Fig. 2a, is composed of three processing steps: 1) membrane pressure layer fabrication, 2) microfluidic layer fabrication, 3) PDMS membrane bonding between the two layers. We fabricated the membrane pressure layer and the microfluidic layer from the PDMS micro-molding process using the 100 μm-thick SU-8 2100 (Microchem, Newton, MA) photoresist mold on silicon wafer (spin rate: 10 s @ 500 rpm, 30 s @ 3000 rpm, exposure time/energy: 6 s @ 20 mW $m^{-2}$ for 120 mJ $cm^{-2}$). A 30 μm-thick PDMS membrane is obtained by the spinning of the PDMS pre-polymer mixture on a silicon wafer for 30 s at 3200 rpm. After the $O_2$ plasma treatment of the PDMS surfaces, the PDMS membrane is sandwiched and bonded between the two layers. Dicing of the 4 × 1 spheroid chip from the bonded layers completes the fabrication process. Fig. 2b shows the fabricated 4 × 1 spheroid chip and the enlarged view of a spheroid well with the dimensions measured from the fabricated device.

### Experimental results and discussion

We use the non-small lung cancer cells of H1650 and supply the cell suspension at the concentration of 2 × $10^6$ $ml^{-1}$ to the inlet port of Fig. 1a. Cells were originally obtained from ATCC. H1650 cells were cultured in T-25 flasks (Greiner, Germany) and maintained in complete media consisting of RPMI-1640 supplemented with 10% (v/v) fetal bovine serum (FBS) and 1% (v/v) penicillin-streptomycin (Invitrogen). The H1650 cells were routinely passaged at 70–80% confluence. The cell culture was maintained in a humidified incubator at 37 °C, 5% $CO_2$, and 100% humidity.

### Cell trapping barriers

From the fabricated devices, we have verified the formation of the cell trapping barrier (Fig. 3a) using the inflated membrane at a pressure of 50 kPa. The cell trapping barrier height, measured as 100 ± 2.5 μm at a membrane pressure of 50 kPa, agrees well with the theoretical value of 99.7 μm estimated from Fig. S1a, ESI.‡

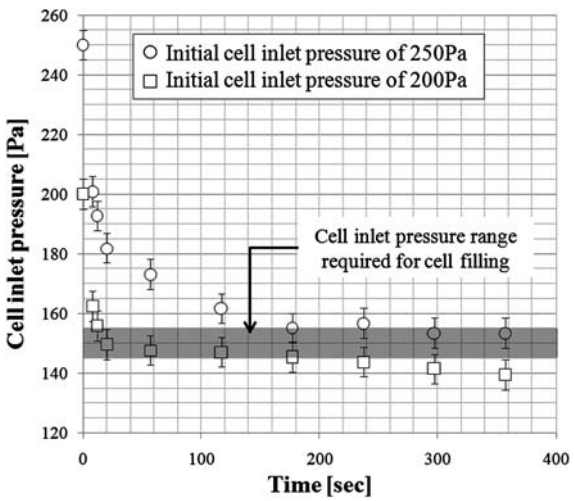


**Fig. 3** Measurement of the cell inlet pressure depending on time for the initial cell inlet pressures of 200 Pa and 250 Pa, respectively: the cell inlet pressure is decreasing from the initial cell inlet pressure, while the hydraulic height, *h* of Fig. 1a, is decreasing from the initial hydraulic height due to the gravity flow of the cell suspension from the inlet port to the outlet port.

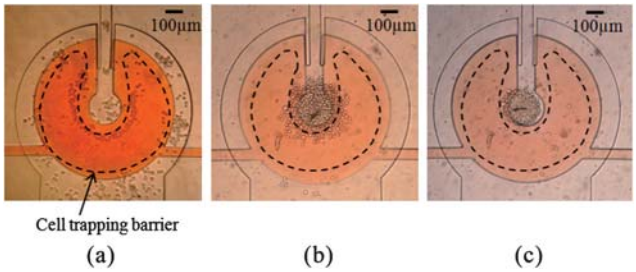


**Fig. 4** Cell trapping, clustering, and spheroid formation within the horseshoe-shaped cell trapping barrier, deformed by the membrane pressure of 50 kPa: (a) initial cell trapping; (b) final cell clustering; and (c) the spheroid formed after 24 h incubation.

### Cell filling and clustering

The cell suspension loaded at the inlet port of Fig. 1a generates the hydraulic pressure due to the height difference between the fluids in the inlet and outlet ports, thus allowing the cells to flow into the 4 × 1 spheroid chip. In Fig. 3, we have monitored the cell inlet pressure depending on time for the initial cell inlet pressures of 200 Pa and 250 Pa, respectively.

We have observed the cell flows near the cell trapping barrier for varying cell inlet pressures. At cell inlet pressures higher than 155 Pa, the cells are bounced out of the cell trapping barrier and are moved directly to the outlet. At inlet pressures lower than 145 Pa, the cell flow was too weak to drive cells into the trapping region. As a result, we observe that the cell inlet pressure required for cell filling is in the range of 145–155 Pa for the fabricated device. Fig. 4 shows the cells initially trapped (Fig. 4a) and the cells finally clustered (Fig. 4b) in the cell trapping region, respectively. After the cell filling, we washed the channel by supplying fresh media solution to the cell inlet port of Fig. 1a.

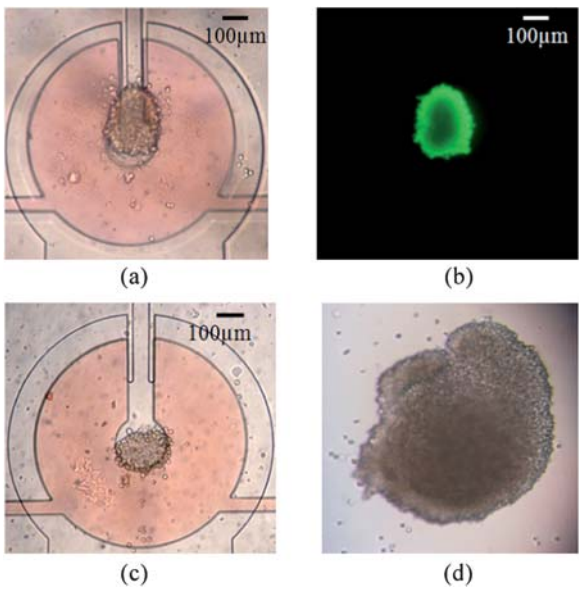


**Fig. 5** Size and viability measurement and spheroid extraction: (a) the bright-field image of the spheroid, from which the edge of the spheroid is detected and the size of the spheroid is measured; (b) the fluorescence image of the spheroid tagged by Calcein-AM probe, from which the viability of the spheroid is verified by green fluorescence; (c) the spheroid formed in the chip; (d) the spheroid extracted from the chip.

### Incubation and spheroid formation

The cell clusters of Fig. 4b formed in the cell trapping barrier are incubated for 24 h in an environment of 5% $CO_2$ and 37 °C, while the membrane pressure is maintained at 50 kPa, thus resulting in the 3D spheroid (Fig. 4c) formed by cell–cell interactions among individual cells. We also observed the viability of the four spheroids formed in the 4 × 1 spheroid chip based on the Calcein-AM cell viability analysis. The green fluorescence image (Fig. 5b) of the spheroid experimentally verifies the viability of the spheroid formed in the spheroid chip.

### Spheroid extraction

We quantitatively measured the cell inlet pressure required for the spheroid extraction by gradually increasing the cell inlet pressure. As a result, we observe that cell inlet pressures of greater than 5 kPa extract the spheroid from the spheroid well without a cell trapping barrier. Fig. 5c shows the spheroid formed in the fabricated chip. It is also observed that the spheroid (Fig. 5d) extracted from the fabricated chip maintains its size and morphology after extraction. For a simple spheroid extraction, pipette aspiration of spheroid solution from the spheroid outlet is also applicable.

### Size and viability characterization

The diameter of the extracted spheroid has been measured by the MATLAB© image processing tool. From the projected area, A, of the spheroids detected from the boundary of spheroids, we obtain the diameter, D. The diameter of the 4 spheroids extracted from the 4 × 1 spheroid chip has been measured as 197.2 ± 11.7 μm, demonstrating the size uniformity within the deviation of 5.9% as well as the size precision within the size error of 1.4% of the spheroids formed and extracted from the 4 × 1 spheroid chip. Additionally, we have data of 195.23 ± 1.66 μm, and 231.38 ± 11.17 μm from different chips with the same conditions, verifying the repeatability and robustness of the device.

We have also characterized the viability of the extracted spheroid. We detach the cells from the extracted spheroids using trypsin EDTA solution and treat the cells with Trypan blue dye. We count the number of the viable cells and measure the percentage of the number of viable cells as 80.3 ± 7.7%. Therefore, we have demonstrated that the present spheroid chip is effective at forming and extracting uniform viable spheroids.

## Conclusions

We have designed, fabricated and characterized a novel 3D spheroid formation and extraction chip using removable cell trapping barriers. The present 4 × 1 spheroid chip has formed and extracted the 3D spheroid in the diameter of 197.2 ± 11.7 μm, maintaining the viability of 80.3 ± 7.7%. The device was designed for only four spheroids to simply verify the possibility of the present spheroid chip. However, by connecting the wells in

 

parallel, we can achieve high-throughput experiments. The inflated cell trapping barrier shows an efficient cell trapping performance at the membrane pressure of 50 kPa for cell inlet pressures of 145–155 Pa. The deflated cell trapping barrier enables us to extract the formed spheroid through outlet ports at the cell inlet pressure of 5 kPa. The present spheroid chip is capable of forming and extracting uniform and precise 3D spheroids within the size deviation of 5.9% and a size error of 1.4%, thus making it possible to use the spheroids for gene expression analysis and cell inoculation in animal models. Furthermore, the present spheroid chip has the possibility of being used for drug screening by culturing the spheroid on chip by perfusion.

## Acknowledgements

This work has been supported by Cell Bench Research Center at KAIST.

## Notes and references

1 D. Cyranoski, *Nature*, 2003, **424**, 870.
2 D. W. Hamer, V. Tilborg, P. Eijk, P. Sminia, D. Troost, V. Noorden, B. Ylstra and S. Leenstra, *Oncogene*, 2008, **27**, 2091.
3 D. Newell, *Br. J. Cancer*, 2001, **84**, 1289.
4 J. M. Kelm, N. E. Timmins, C. J. Brown, M. Fussenegger and L. K. Nielsen, *Biotechnol. Bioeng.*, 2003, **83**, 174.
5 R. M. Enmon Jr, K. C. O'Connor, D. J. Lacks, D. K. Schwartz and R. S. Dotson, *Biotechnol. Bioeng.*, 2001, **72**, 579.
6 J. Fukuda and K. Nakazawa, *Tissue Eng.*, 2005, **11**, 1254.
7 Y. l. Torisawa, A. Takagi, Y. Nashimoto, T. Yasukawa, H. Shiku and T. Matsue, *Biomaterials*, 2007, **28**, 559.
8 A. Khademhosseini, J. Yeh, S. Jon, G. Eng, K. Y. Suh, J. A. Burdick and R. Langer, *Lab Chip*, 2004, **4**, 425.
9 L. Y. Wu, D. D. Carlo and L. P. Lee, *Biomed. Microdevices*, 2008, **10**, 197.
10 T. Tamura, Y. Sakai and K. Nakazawa, *J. Mater. Sci.: Mater. Med.*, 2008, **19**, 2071.
11 Y. Torisawa, B. Chueh, D. Huh, P. Ramamurthy, T. M. Roth, K. F. Barald and S. Takayama, *Lab Chip*, 2007, **7**, 770.
12 A. Y. Hsiao, Y. Torisawa, Y. Tung, S. Sud, R. S. Taichman, K. J. Pienta and S. Takayama, *Biomaterials*, 2009, **30**, 3020.
13 T. Thorsen, S. J. Maerkl and S. R. Quake, *Science*, 2002, **298**, 580.
14 J. Friedrich, C. Seidel, R. Ebner and L. A. Kunz-Schughart, *Nat. Protoc.*, 2009, **4**, 309.
15 K. Suzuki, and B. W. Smith, *Microlithography: science and technology*, Taylor & Francis, London, 2nd edn, 2007.
16 A. lvascu and M. Kubbies, *J. Biomol. Screening*, 2006, **11**, 992.
17 H. Acker, *J. Theor, Med.*, 1998, **1**, 193.
18 D. Newell, *Br. J. Cancer*, 2001, **84**, 1289.
19 Y. Shafrana and N. Zurgil, *Lab Chip*, 2006, **6**, 995.
20 D. Di Carlo, L. Y. Wu and L. P. Lee, *Lab Chip*, 2006, **6**, 1445.
21 L. Kim, M. D. Vahey, H. Lee and J. Voldman, *Lab Chip*, 2006, **6**, 394.
22 A. Tourovskaia, X. Figueroa-Masot and A. Folch, *Lab Chip*, 2005, **5**, 14.
23 D. Di Carlo, N. Aghdam and L. P. Lee, *Anal. Chem.*, 2006, **78**, 4925.
24 D. M. Thompson, K. R. King, K. J. Wieder, M. Toner, M. L. Yarmush and A. Jayaraman, *Anal. Chem.*, 2004, **76**, 4098.
25 B. Desoize, *Crit. Rev. Oncol. Hematol.*, 2000, **36**, 59–60.
26 R. C. Bates, N. S. Edwards and J. D. Yates, *Crit. Rev. Oncol. Hematol.*, 2000, **36**, 61.
27 G. M. Keller, *Curr. Opin. Cell Biol.*, 1995, **7**, 862.
28 M. A. Faute, L. Laurent, D. Ploton, M. F. Poupon, J. C. Jardillier and H. Bobichon, *Clin. Exp. Metastasis*, 2002, **19**, 161.
29 P. L. Olive and R. E. Durand, *Cancer Metastasis Rev.*, 1994, **13**, 121.